

# Brain Tumor Segmentation and Tractographic Feature Extraction from Structural MR Images for Overall Survival Prediction

Po-Yu Kao<sup>1</sup>, Thuyen Ngo<sup>1</sup>, Angela Zhang<sup>1</sup>,  
Jefferson Chen<sup>2</sup>, and B.S. Manjunath<sup>1</sup>

<sup>1</sup> Vision Research Lab, University of California, Santa Barbara, CA, USA  
poyu\_kao@ece.ucsb.edu

<sup>2</sup> UC Irvine Health, University of California, Irvine, CA, USA

**Abstract.** This paper introduces a novel methodology to integrate human brain connectomics and parcellation for tumor segmentation and survival prediction. For segmentation, we utilize an existing brain parcellation atlas in the MNI152 1mm space and map the parcellation to each individual subject data. We leverage current state-of-the-art deep networks together with hard negative mining to achieve the final voxel level classification. This method achieves mean Dice scores of 0.904, 0.785 and 0.805 on segmentation of the whole tumor, tumor core and enhancing tumor, respectively. For survival prediction, we present a new method for combining features from connectomics data, brain parcellation, and the segmented brain tumor. Since the BraTS dataset does not include diffusion tensor imaging data for computing tractography, we use the average connectome information from the Human Connectome Project and map each subject brain volume onto this common connectome space. From this, we compute tractographic features that describe potential disruptions due to the brain tumor. These features are then used to predict the overall survival time. The proposed tractographic features achieve an average accuracy of 69% on training data and 50% on validation data.

**Keywords:** Brain Tumor Segmentation · Hard Negative Mining · Ensemble Modeling · Overall Survival Prediction · Tractographic Feature · Support Vector Machine

## 1 Introduction

Glioblastomas, or Gliomas, are one of the most common types of brain tumor. They have a highly heterogeneous appearance and shape and may happen at any location in the brain. High-Grade Glioma (HGG) is one of the most aggressive types of brain tumor with median survival of 15 months [15]. In [9], seven different 3D neural network models including two DeepMedics [10], three 3D FCNs [11] and two 3D U-Nets [4] with different parameters are combined, and the output probability maps from each model are averaged to obtain the final brain tumor mask. In [17], a hierarchical pipeline is designed to segment the

different types of tumor compartments using anisotropic convolutional neural networks. The network architecture in [6] is derived from a 3D U-Net with additional residual connections on context pathway and additional multi-scale aggregation on localization pathways, using the Dice loss in the training phase to circumvent class imbalance. For the brain tumor segmentation task, we propose a methodology to integrate multiple DeepMedics and 3D U-Nets in order to get a robust brain tumor segmentation in multimodal structural MR images. We also utilize the brain parcellation to bring the location information to DeepMedic. In order to increase the diversity of our ensemble, 3D U-Nets with dice loss and cross-entropy loss are included. A hard negative mining strategy is used while we train a 3D U-Net, with cross-entropy loss to mitigate class imbalance. The final segmentation mask of the brain tumor is calculated by taking the average of the output probability maps from each model in our ensemble.

In addition, we design a system to automatically extract important features from gliomas and predict the overall survival (OS) for glioma patients. In [14], they extracts 40 features from the predicted brain tumor mask and uses a random forest regression to predict the glioma patient's OS. In [8], four features are extracted from each subject and a support vector machine (SVM) with Radial Basis Function (RBF) kernel is used to classify glioma patients into three different OS groups. In this paper, we propose a method to extract the tractographic features from the lesion regions on structural MR images via a average diffusion MR image which is averaged from a total of 1021 subjects (Q1-Q4, 2017). The volumetric features, spatial features, and morphological features are also extracted from these lesion regions. We use these lesion-related features along with age to predict the OS using a Support Vector Machine (SVM) classifier.

## 2 Task 1: Segmentation of Gliomas in Pre-operative MRI Scans

### 2.1 Materials

The Brain Tumor Segmentation (BraTS) 2018 dataset [1,2,3,12] provides 285 training subjects with four different types of MR images (MR-T1, MR-T1ce, MR-T2 and MR-FLAIR) and expert-labeled ground truths of lesions, including necrosis, non-enhancing tumor, edema, and enhancing tumor. The dataset also offers 66 validation subjects with four different types of MR images and is distributed after pre-processing - i.e. co-registration to the same anatomical template, interpolated to the same resolution ( $1mm^3$ ) and skull-stripped.

### 2.2 Data Pre-processing

Data normalization is a crucial step before training the deep neural network. We need to make sure the inputs have the same scale in order to speed up the training process and improve the network's performance. For each subject, we apply Z-score normalization within the brain regions for each type of MR image.

### 2.3 Network Architecture and Training

Our proposed ensemble combines eight 3D neural networks based on 3D U-Net [4] and DeepMedic [10]. In our ensemble, we have one original DeepMedic and four modified DeepMedics with different numbers of convolutional kernels and training parameters. The original DeepMedic does not consider the location information of each input patch inside the brain. We bring this location information to the network by creating 21 binary Harvard-Oxford subcortical brain parcellation masks [5] in the subject space as additional inputs to the neural network. We call this model DeepMedic-c25. We also train one DeepMedic with 24 additional brain parcellation channels and no data augmentation. We call this model DeepMedic-c25-n. A DeepMedic with double convolutional kernels, called DeepMedic-double and a DeepMedic with triple convolutional kernels, called DeepMedic-triple are included in our ensemble.

Our ensemble also has three 3D U-Nets, including one revised version of [6] with group normalization [18] and two 3D U-Nets, named 3D-UNet-ce-1 and 3D-UNet-ce-2 with cross-entropy loss. The 3D U-Net in [6] are trained using Dice loss in order to solve the class imbalance problem in the BraTS 2017 challenge. However, in order to increase the diversity of our ensemble, we also include two 3D U-Nets trained using cross-entropy loss. We utilize a hard negative mining strategy to solve the class imbalance problem while we train 3D U-Nets with the cross-entropy loss. In the end, we take the average of the output probability maps from each model and get the final brain tumor segmentation.

**Hard Negative Mining** We train 3D U-Nets with 128x128x128 patches randomly cropped from the original data. With such large dimensions, the majority of pixels are not classified as lesion and standard cross-entropy loss would encourage the model to favor the background class. To cope with this problem, we only select negative pixels with the largest losses (hard negative) to back-propagate the gradients. In our implementation the number of selected negative pixels is at most three times the number of positive pixels. Hard negative mining not only improves the performance of our classifier but also decreases its false positive rate.

### 2.4 Result

In this task, we compare the performance of our ensemble with each individual model. The quantitative results are shown in Table 1.

## 3 Task 2: Prediction of Patient Overall Survival from Pre-operative MRI Scans

### 3.1 Material

In addition to the data used in the brain segmentation challenge, the age (in years), survival (in days) and resection status are provided for 163 subjects in

**Table 1.** Quantitative results of the individual model and our ensemble on BraTS 2018 validation dataset (reported as mean  $\pm$  one standard deviation). Bold numbers highlight the best result for a given metric and tumor compartments (ET: enhancing tumor, WT: whole tumor, and TC: tumor core)

	Model	ET	WT	TC
<i>Dice</i>	DeepMedic	0.772 $\pm$ 0.248	0.897 $\pm$ 0.071	0.801 $\pm$ 0.219
	DeepMedic-c25	0.752 $\pm$ 0.280	0.895 $\pm$ 0.064	0.805 $\pm$ 0.230
	DeepMedic-c25-n	0.766 $\pm$ 0.261	0.893 $\pm$ 0.070	0.788 $\pm$ 0.244
	DeepMedic-double	0.757 $\pm$ 0.260	0.893 $\pm$ 0.088	0.782 $\pm$ 0.231
	DeepMedic-triple	0.777 $\pm$ 0.236	0.895 $\pm$ 0.085	0.792 $\pm$ 0.230
	3D U-Net	0.770 $\pm$ 0.251	0.892 $\pm$ 0.060	0.770 $\pm$ 0.224
	3D-UNet-ce-1	0.745 $\pm$ 0.271	0.884 $\pm$ 0.127	0.768 $\pm$ 0.222
	3D-UNet-ce-2	0.745 $\pm$ 0.269	0.891 $\pm$ 0.110	0.760 $\pm$ 0.244
	Our ensemble	<b>0.785<math>\pm</math> 0.248</b>	<b>0.904<math>\pm</math> 0.073</b>	<b>0.805<math>\pm</math> 0.218</b>
	DeepMedic	<b>0.816<math>\pm</math> 0.217</b>	0.919 $\pm$ 0.089	0.802 $\pm$ 0.217
<i>Sensitivity</i>	DeepMedic-c25	0.803 $\pm$ 0.250	<b>0.925<math>\pm</math> 0.072</b>	0.794 $\pm$ 0.248
	DeepMedic-c25-n	0.806 $\pm$ 0.244	0.918 $\pm$ 0.092	0.792 $\pm$ 0.251
	DeepMedic-double	0.794 $\pm$ 0.235	0.913 $\pm$ 0.113	0.801 $\pm$ 0.225
	DeepMedic-triple	0.800 $\pm$ 0.230	0.911 $\pm$ 0.110	0.789 $\pm$ 0.243
	3D U-Net	0.784 $\pm$ 0.248	0.919 $\pm$ 0.085	0.791 $\pm$ 0.245
	3D-UNet-ce-1	0.785 $\pm$ 0.249	0.896 $\pm$ 0.160	0.791 $\pm$ 0.230
	3D-UNet-ce-2	0.802 $\pm$ 0.251	0.904 $\pm$ 0.133	<b>0.803<math>\pm</math> 0.249</b>
	Our ensemble	0.806 $\pm$ 0.245	0.918 $\pm$ 0.102	0.795 $\pm$ 0.236
	DeepMedic	0.998 $\pm$ 0.004	0.994 $\pm$ 0.005	0.997 $\pm$ 0.004
	DeepMedic-c25	0.998 $\pm$ 0.003	0.993 $\pm$ 0.006	0.998 $\pm$ 0.003
<i>Specificity</i>	DeepMedic-c25-n	0.998 $\pm$ 0.004	0.993 $\pm$ 0.005	0.997 $\pm$ 0.004
	DeepMedic-double	0.998 $\pm$ 0.003	0.993 $\pm$ 0.005	0.997 $\pm$ 0.004
	DeepMedic-triple	0.998 $\pm$ 0.004	0.993 $\pm$ 0.005	0.997 $\pm$ 0.003
	3D U-Net	0.998 $\pm$ 0.003	0.993 $\pm$ 0.005	0.997 $\pm$ 0.003
	3D-UNet-ce-1	0.998 $\pm$ 0.003	0.994 $\pm$ 0.006	0.996 $\pm$ 0.007
	3D-UNet-ce-2	0.998 $\pm$ 0.003	0.994 $\pm$ 0.005	0.996 $\pm$ 0.004
	Our ensemble	0.998 $\pm$ 0.003	0.994 $\pm$ 0.005	0.998 $\pm$ 0.003
	DeepMedic	4.723 $\pm$ 9.018	6.290 $\pm$ 5.570	9.181 $\pm$ 13.612
	DeepMedic-c25	<b>3.376<math>\pm</math> 4.918</b>	<b>10.992<math>\pm</math> 18.590</b>	<b>9.902<math>\pm</math> 18.277</b>
	DeepMedic-c25-n	4.108 $\pm$ 5.920	8.682 $\pm$ 11.907	9.928 $\pm$ 14.247
<i>Hausdorff95 (in mm)</i>	DeepMedic-double	4.696 $\pm$ 8.683	5.969 $\pm$ 7.631	10.919 $\pm$ 17.270
	DeepMedic-triple	5.826 $\pm$ 12.333	6.583 $\pm$ 9.590	9.787 $\pm$ 12.743
	3D U-Net	4.180 $\pm$ 7.920	5.657 $\pm$ 7.353	10.641 $\pm$ 14.207
	3D-UNet-ce-1	4.416 $\pm$ 7.850	5.627 $\pm$ 7.609	10.127 $\pm$ 13.655
	3D-UNet-ce-2	5.956 $\pm$ 11.858	4.726 $\pm$ 4.435	10.882 $\pm$ 15.407
	Our ensemble	3.744 $\pm$ 7.832	<b>3.946<math>\pm</math> 3.166</b>	<b>7.833<math>\pm</math> 13.076</b>

the training dataset. 59 of them have resection status of Gross Total Resection (GTR). The validation dataset has 53 subjects with age (in years) and resection status. 28 of them have resection status GTR. For this task we predict the overall survival (OS) for glioma patients with resection status of GTR.

### 3.2 Methodology

Our proposed pipeline, shown in Figure 1, includes three stages: In the first stage, we use all structural MR images from each subject to obtain the predicted lesion mask for each subject. We then extract five different types of features from each subject. Four of them are from the predicted lesion mask, and the remaining one is the subject's age. In the second stage, we perform feature concatenation, feature normalization, and feature selection. In the final stage, we train a classifier using the features extracted from the training subjects and evaluate its performance on the validation subjects.

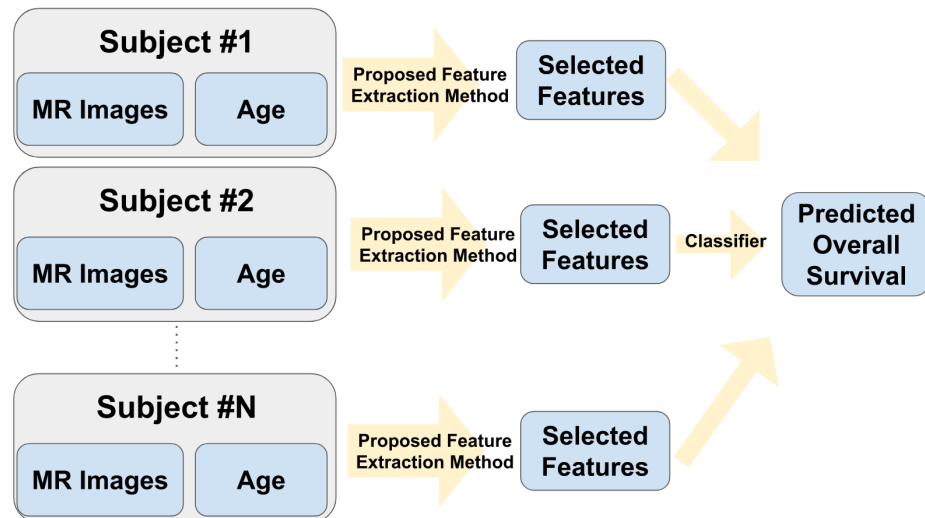
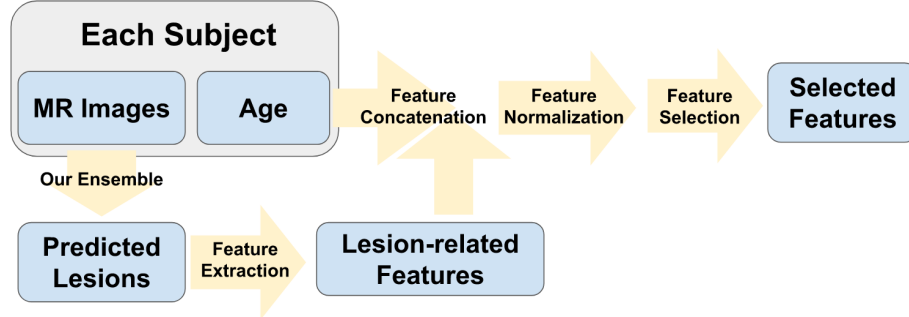


Fig. 1. Overall survival classification pipeline.

**Glioma Segmentation:** To segment the gliomas, we use the proposed method in the previous section to obtain the prediction of three different tissue types which includes necrosis, non-enhancing tumor, edema, and enhancing tumor.

**Feature Extraction from the Glioma Segmentation:** After we obtain the predicted lesion mask, we extract four different types of features from this mask for each subject. These features include volumetric features, spatial features,

morphological features, and tractographic features. For each subject, we extract approximately 800 features. The feature extraction pipeline for one subject is shown in Figure 2.



**Fig. 2.** Feature extraction pipeline for one subject.

*Volumetric Features:* The volumetric features include the volume and the ratio of brain to the different types of lesions, as well as the tumor compartments. We have 19 volumetric features from each subject.

*Spatial Features:* The spatial features describe the location of the tumor in the brain. We extract the centroids and volumes of different types of tumor tissue in each of the Harvard-Oxford subcortical structural atlas brain parcellation regions. FMRIB's Linear Image Registration Tool (FLIRT) [7] is used to map the Harvard-Oxford subcortical structural atlas from the MNI152 1mm space to each individual's subject space. For each subject, we extract around 90 spatial features.

*Morphological Features:* The morphological features include the length of the major axis of the lesion, the length of the minor axis of the lesion and the surface irregularity of the lesions. We extract 19 morphological features from each subject.

*Tractographic Features:* Tractographic features describe the potentially damaged parcellation regions impacted by the brain tumor through fiber tracking. Figure 3 shows the workflow for building a connectivity matrix for each subject. First, the predicted whole tumor mask and the average diffusion orientation distribution function from HCP-1021, created by QSDR [19], are obtained for each subject. FLIRT is used to map the whole tumor mask from subject space to MNI152 1mm space. Second, we use a deterministic diffusion fiber tracking method [20] to create approximately 1,000,000 tracts from the whole tumor

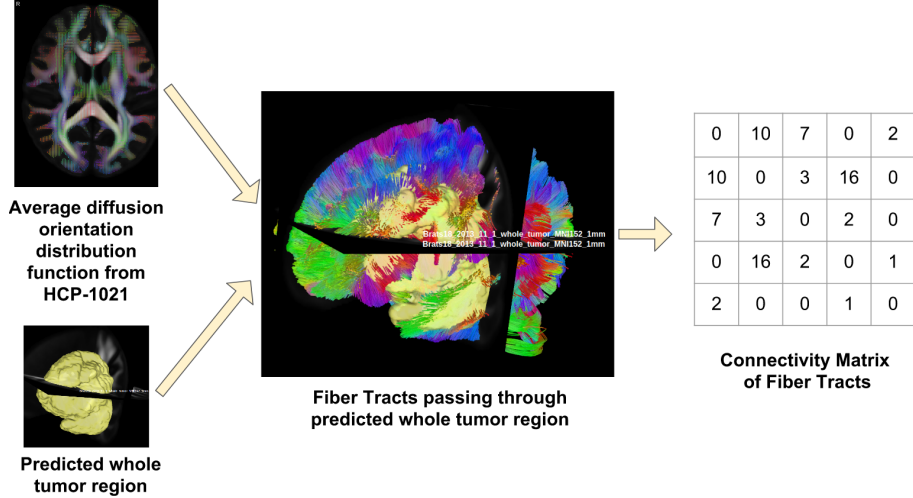


**Fig. 3.** Workflow for building a connectivity matrix for each subject. ITK-SNAP [21] is used for visualizing the 3D MR images and 3D labels.

region. Finally, a structural brain atlas is used to create a connectivity matrix  $W_{ori}$  for each subject. This matrix contains information about whether a fiber connecting one region to another passed through or ended at those regions, as shown:

$W_{ori}$  is a  $N \times N$  matrix, and  $N$  is the number of parcellation in a structural brain atlas.

$$W_{ori} = \begin{bmatrix} w_{ori,11} & w_{ori,12} & \dots & w_{ori,1N} \\ w_{ori,21} & w_{ori,22} & \dots & w_{ori,2N} \\ \vdots & \vdots & \ddots & \vdots \\ w_{ori,N1} & w_{ori,N2} & \dots & w_{ori,NN} \end{bmatrix} \quad (1)$$

If  $w_{ij}$  is pass type, it shows the number of tracts passing through region  $j$  and region  $i$ . If  $w_{ij}$  is end type, it shows the number of tracts starting from a region  $i$  and ending in a region  $j$ . From the original connectivity matrix  $W_{ori}$ , we create a normalized version  $W_{nrm}$  and a binarized version  $W_{bin}$ .

$$W_{nrm} = W_{ori} / \max(W_{ori}) \quad (2)$$

$/$  is the element-wise division operator and  $\max(W_{ori})$  is the maximum value of the original connectivity matrix  $W_{ori}$ .

$$W_{bin} = \begin{bmatrix} w_{bin,11} & w_{bin,12} & \dots & w_{bin,1N} \\ w_{bin,21} & w_{bin,22} & \dots & w_{bin,2N} \\ \vdots & \vdots & \ddots & \vdots \\ w_{bin,N1} & w_{bin,N2} & \dots & w_{bin,NN} \end{bmatrix} \quad (3)$$

$w_{bin,ij} = 0$  if  $w_{ori,ij} = 0$ , and  $w_{bin,ij} = 1$  if  $w_{ori,ij} > 0$ . Then, we sum up each column in a connectivity matrix to form a tractographic feature vector.

$$\mathbf{V} = \sum_{i=1}^N w_{ij} = [v_1, v_2, \dots, v_N] \quad (4)$$

Furthermore, we weight every element in the tractographic feature vector with respect to the ratio of the lesion in a brain parcellation region to the volume of this brain parcellation region.

$$\mathbf{V}_{wei} = \boldsymbol{\alpha} \odot \mathbf{V}, \boldsymbol{\alpha} = [t_1/b_1, t_2/b_2, \dots, t_N/b_N] \quad (5)$$

$\odot$  is the element-wise multiplication operator,  $t_i$  is the volume of the whole brain tumor in the  $i$ -th brain parcellation, and  $b_i$  is the volume of the  $i$ -th brain parcellation. Automated Anatomical Labeling (AAL) [16] is used, so the dimension of the connectivity matrix  $\mathbf{W}$  is  $116 \times 116$ . In the end, we extract six tractographic feature vectors from each subject which have 696 dimensions.

**Feature Concatenation, Normalization and Selection:** We concatenate all of the obtained features together with subject's age to form a final high dimensional feature vector for each subject. Then, we remove features that have low variance between subjects and apply z-score normalization on the remaining features. In the feature selection step, we combine recursive feature elimination with the repeated stratified K-fold cross validator. These feature processing steps are implemented by using scikit-learn [13].

**Prediction of Patient Overall Survival:** We first divide all 59 training subjects into three groups: long-survivors (e.g.,  $>15$  months), short-survivors (e.g.,  $<10$  months), and mid-survivors (e.g., between 10 and 15 months). Then, we train an SVM on all training subjects. Finally, we obtain predicted labels for the validation subjects and upload them to the evaluation website.

### 3.3 Results

In the overall survival prediction task, we examine the performance of each type of feature compared to combined features. The ground truth of lesions are used to extract four different types of features. Recursive feature elimination and cross-validated selection (RFECV) are used in the feature selection step, and a Support Vector Machine (SVM) is trained with 1000-times repeated stratified 5-folds cross-validator. The classification accuracy with one standard deviation for the training dataset is shown in Figure 4. By only using the tractographic features with RCV and a SVM classifier, the classification accuracy is 0.5 in the validation dataset. However, the classification accuracy drops to 0.429 when we use all combined features with RFECV and a SVM classifier in the validation dataset.

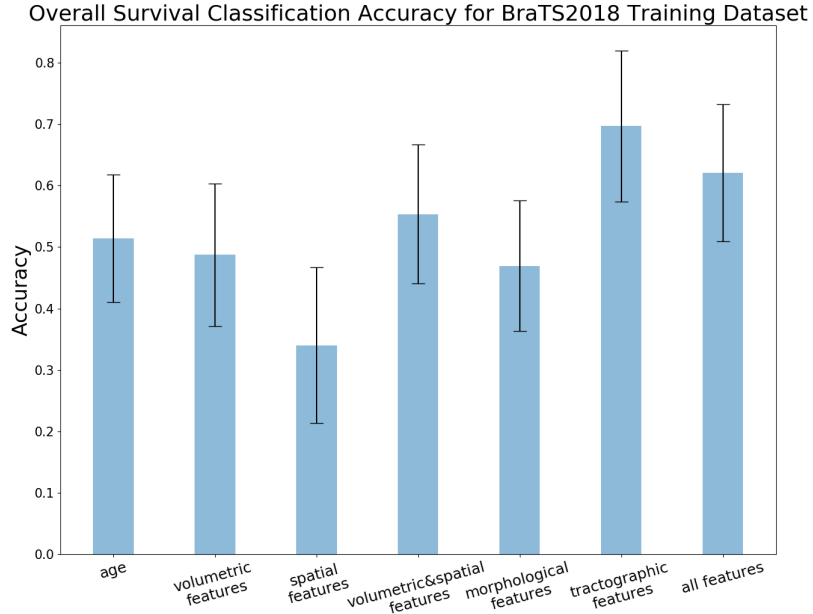


**Fig. 4.** Classification accuracy between each different types of features and all combined features. We consider the volume of different types of lesions in different brain parcellation regions as volumetric&spatial features.

## 4 Discussion

For the brain tumor segmentation task, our ensemble has better performance on all *Dice* scores for all tumor compartments compared to each individual model. It also has better performance on *Hausdorff* distances for the whole tumor and tumor core. *Specificity* (also called the true negative rate) are pretty similar between each individual model and our ensemble due to the class imbalance of the foreground and the background.

DeepMedic with 21 more binary brain parcellation channels has better performance on the *sensitivity* (also called the true positive rate) of whole tumor region and the *Hausdorff* distance of enhancing tumor region compared to other models and our ensemble. Original DeepMedic has a better performance on the *sensitivity* of enhancing tumor region, and the 3D U-Net which is train by cross-entropy loss has a better performance on the *sensitivity* of tumor core region compared to our ensemble and other models.

For the overall survival prediction task, the 12 selected tractographic features achieve 69 % classification accuracy which is better than other types of features and the combined features. These tractographic features are from the left precentral gyrus, right precentral gyrus, left insula, right insula, right mid-

cingulate area, left posterior cingulate gyrus, left superior occipital gyrus, right fusiform gyrus, right globus pallidus, right middle temporal pole, left inferior temporal gyrus and right inferior temporal gyrus. These regions are the key regions to affect the brain tumor patient's survival period.

The features we used to report the classification accuracy in Figure 4 are from the ground truth lesions. We repeat 5-fold cross-validation 1000 times to train a SVM classifier with different types of features and all combined features in order to find more reliable features. The tractographic features has the best performance among other different types of feature and the combined features.

However, when we evaluate the tractographic features which are extracted from the predicted tumor segmentation, the classification accuracy drops to 0.5. We believe this drop is due to the imperfection of our tumor segmentation tool.

## 5 Conclusions

Our proposed ensemble has the best performance on the *Dice* scores of the whole tumor, tumor core and enhancing tumor and the smallest *Hausdorff* distance in the whole tumor and tumor core compared to each individual model. It is shown that increasing the number of model and the diversity of model in our ensemble results in a more robust tumor segmentation.

Our proposed tractographic features are reliable features to predict the overall survival for the tumor patients. The following 12 regions are the pivotal: left precentral gyrus, right precentral gyrus, left insula, right insula, right midcingulate area, left posterior cingulate gyrus, left superior occipital gyrus, right fusiform gyrus, right globus pallidus, right middle temporal pole, left inferior temporal gyrus and right inferior temporal gyrus. The tumor spreading in these 12 regions has a greater impact on patient's overall survival compared to other regions inside the brain.

## References

1. Bakas, S., Akbari, H., Sotiras, A., Bilello, M., Rozycski, M., Kirby, J., Freymann, J., Farahani, K., Davatzikos, C.: Segmentation labels and radiomic features for the pre-operative scans of the tcga-lgg collection. *The Cancer Imaging Archive*. (2017). <https://doi.org/10.7937/K9/TCIA.2017.GJQ7R0EF>
2. Bakas, S., Akbari, H., Sotiras, A., Bilello, M., Rozycski, M., Kirby, J., Freymann, J., Farahani, K., Davatzikos, C.: Segmentation labels and radiomic features for the pre-operative scans of the tcga-gbm collection. *The Cancer Imaging Archive*. (2017). <https://doi.org/10.7937/K9/TCIA.2017.KLXWJJ1Q>
3. Bakas, S., Akbari, H., Sotiras, A., Bilello, M., Rozycski, M., Kirby, J.S., Freymann, J.B., Farahani, K., Davatzikos, C.: Advancing the cancer genome atlas glioma mri collections with expert segmentation labels and radiomic features. *Scientific data* **4**, 170117 (2017)
4. Çiçek, Ö., Abdulkadir, A., Lienkamp, S.S., Brox, T., Ronneberger, O.: 3d u-net: learning dense volumetric segmentation from sparse annotation. In: *International Conference on Medical Image Computing and Computer-Assisted Intervention*. pp. 424–432. Springer (2016)

5. Desikan, R.S., Ségonne, F., Fischl, B., Quinn, B.T., Dickerson, B.C., Blacker, D., Buckner, R.L., Dale, A.M., Maguire, R.P., Hyman, B.T., et al.: An automated labeling system for subdividing the human cerebral cortex on mri scans into gyral based regions of interest. *Neuroimage* **31**(3), 968–980 (2006)
6. Isensee, F., Kickingereder, P., Wick, W., Bendszus, M., Maier-Hein, K.H.: Brain tumor segmentation and radiomics survival prediction: Contribution to the brats 2017 challenge. In: International MICCAI Brainlesion Workshop. pp. 287–297. Springer (2017)
7. Jenkinson, M., Smith, S.: A global optimisation method for robust affine registration of brain images. *Medical image analysis* **5**(2), 143–156 (2001)
8. Jungo, A., McKinley, R., Meier, R., Knecht, U., Vera, L., Pérez-Beteta, J., Molina-García, D., Pérez-García, V.M., Wiest, R., Reyes, M.: Towards uncertainty-assisted brain tumor segmentation and survival prediction. In: International MICCAI Brainlesion Workshop. pp. 474–485. Springer (2017)
9. Kamnitsas, K., Bai, W., Ferrante, E., McDonagh, S., Sinclair, M., Pawlowski, N., Rajchl, M., Lee, M., Kainz, B., Rueckert, D., et al.: Ensembles of multiple models and architectures for robust brain tumour segmentation. In: International MICCAI Brainlesion Workshop. pp. 450–462. Springer (2017)
10. Kamnitsas, K., Ledig, C., Newcombe, V.F., Simpson, J.P., Kane, A.D., Menon, D.K., Rueckert, D., Glocker, B.: Efficient multi-scale 3d cnn with fully connected crf for accurate brain lesion segmentation. *Medical image analysis* **36**, 61–78 (2017)
11. Long, J., Shelhamer, E., Darrell, T.: Fully convolutional networks for semantic segmentation. In: Proceedings of the IEEE conference on computer vision and pattern recognition. pp. 3431–3440 (2015)
12. Menze, B.H., Jakab, A., Bauer, S., Kalpathy-Cramer, J., Farahani, K., Kirby, J., Burren, Y., Porz, N., Slotboom, J., Wiest, R., et al.: The multimodal brain tumor image segmentation benchmark (brats). *IEEE transactions on medical imaging* **34**(10), 1993 (2015)
13. Pedregosa, F., Varoquaux, G., Gramfort, A., Michel, V., Thirion, B., Grisel, O., Blondel, M., Prettenhofer, P., Weiss, R., Dubourg, V., Vanderplas, J., Passos, A., Cournapeau, D., Brucher, M., Perrot, M., Duchesnay, E.: Scikit-learn: Machine learning in Python. *Journal of Machine Learning Research* **12**, 2825–2830 (2011)
14. Shboul, Z.A., Vidyaratne, L., Alam, M., Iftekharuddin, K.M.: Glioblastoma and survival prediction. In: International MICCAI Brainlesion Workshop. pp. 358–368. Springer (2017)
15. Thakkar, J.P., Dolecek, T.A., Horbinski, C., Ostrom, Q.T., Lightner, D.D., Barnholtz-Sloan, J.S., Villano, J.L.: Epidemiologic and molecular prognostic review of glioblastoma. *Cancer Epidemiology and Prevention Biomarkers* (2014)
16. Tzourio-Mazoyer, N., Landeau, B., Papathanassiou, D., Crivello, F., Etard, O., Delcroix, N., Mazoyer, B., Joliot, M.: Automated anatomical labeling of activations in spm using a macroscopic anatomical parcellation of the mri mri single-subject brain. *Neuroimage* **15**(1), 273–289 (2002)
17. Wang, G., Li, W., Ourselin, S., Vercauteren, T.: Automatic brain tumor segmentation using cascaded anisotropic convolutional neural networks. In: International MICCAI Brainlesion Workshop. pp. 178–190. Springer (2017)
18. Wu, Y., He, K.: Group normalization. arXiv preprint arXiv:1803.08494 (2018)
19. Yeh, F.C., Tseng, W.Y.I.: Ntu-90: a high angular resolution brain atlas constructed by q-space diffeomorphic reconstruction. *Neuroimage* **58**(1), 91–99 (2011)
20. Yeh, F.C., Verstynen, T.D., Wang, Y., Fernández-Miranda, J.C., Tseng, W.Y.I.: Deterministic diffusion fiber tracking improved by quantitative anisotropy. *PloS one* **8**(11), e80713 (2013)

21. Yushkevich, P.A., Piven, J., Cody Hazlett, H., Gimpel Smith, R., Ho, S., Gee, J.C., Gerig, G.: User-guided 3D active contour segmentation of anatomical structures: Significantly improved efficiency and reliability. *Neuroimage* **31**(3), 1116–1128 (2006)